Characterization of reflectivity inversion, α- and β-phase transitions and nanostructure formation in hydrogen activated thin Pd films on silicon based substrates

K. Kalli,[a] A. Othonos, and C. Christofides
Department of Physics, University of Cyprus, P. O. Box 20537, Nicosia 1678, Cyprus

(Received 6 November 2000; accepted for publication 18 September 2001)

Optically thin palladium metal films evaporated on different silicon based substrates are investigated following exposure to different concentrations of hydrogen gas in air. Laser modulated reflectance off the palladium surface of silicon oxide and silicon nitride substrates is used to recover information regarding the reflectivity inversion and α/β-phases of the palladium complex after both first and multiple gas cycling. Atomic force microscopy confirms the formation of metal nanostructures following exposure to hydrogen of the optically thin palladium films. © *2002 American Institute of Physics.* [DOI: 10.1063/1.1417992]

I. INTRODUCTION

The H–Pd system has received extensive interest primarily from the use of Pd as a catalyst that results from its unusual property of being able to absorb up to 900 times its own volume with hydrogen at room temperature. This makes Pd an efficient storage medium for hydrogen and its isotopes.[1,2] As a result of this absorption, the Pd undergoes structural changes through the formation of Pd hydride, PdH_x. The process of the hydride formation is driven by surface adsorption, through chemisorption, followed by absorption through the Pd volume, after which the system reaches equilibrium at the various interfaces, namely, gas-Pd and Pd substrate, and within the Pd bulk.

With the development of semiconductor technology and silicon based integration of devices, it is important to investigate metal films evaporated on silicon substrates, particularly when the thin metal films offer additional properties arising from structural changes on nanometer scales. We investigate the exposure to hydrogen of Pd metal thin films evaporated on various silicon-based substrates; specifically, optically thin films of Pd evaporated on amorphous silicon dioxide on crystalline silicon and silicon nitride on a crystalline silicon support. Of particular interest are the surface structural changes observed in Pd, formed following hydrogen exposure. These changes constitute Pd clusters of nanometer scale, which are examined using an atomic force microscope (AFM). The optically thin Pd films range from 1 nm, corresponding to extremely small island-like structures, to 10 nm matrix structures, where large-scale coalescence occurs and finally as continuous films, several tens of nanometers thick.

A. Pd on silicon

The most characteristic room temperature phenomenon is the α to β phase transition. In the early stages of hydrogen adsorption/absorption (α phase), hydrogen atoms randomly populate small interstices in the lattice structure, with the concentration of hydrogen atoms increasing until at a critical point (β phase) the lattice expands, further inducing hydrogen to cluster at much higher densities. The lattice constant change, as hydrogen enters the metal, can reach a maximum of 3% in length or 10% in volume in the β phase.[1] This process is considered reversible, thus when hydrogen escapes, the metal returns to its original state.

The exact degree of coverage depends on many factors, such as temperature and pressure and, in the case where the Pd is deposited on a supporting structure, on the uniformity of the deposition method and the change in surface energy of the system on gas cycling. At low concentrations (α phase), the dissolved hydrogen behaves according to Sievert's law, where the H to Pd atomic ratio, $n = K_s p^{1/2}$, with K_s = Sievert's constant.[3] The compositions for which α and β phases coexist at 25 °C lie between $n = 0.015$ and 0.58. According to Lewis, in both phases the Pd lattice is face-centered-cubic (fcc) with the hydrogen atoms located in the octahedral interstices.[1]

The bulk behavior of the H–Pd system is well characterized, yet very little work has been done for thin metal films (less than a few tens of nanometers). Abnormal and interesting properties are expected since outer surface effects and changes in optical thickness are complicated by the influence of the second boundary layer at the insulator–metal interface and by the morphological changes of the optically thin metal. Any changes that may occur, on exposure of the Pd system to hydrogen gas, are a combination of the surface effects, morphological changes, and index of refraction changes of the bulk (which include thickness changes of Pd).

B. Optically thick and thin films

Electrical measurements are employed to measure changes in the physical properties of continuous (>100 nm) Pd films through either resistance changes,[4] or via capacitance measurements, for example on Pd–metal silicon dioxide on silicon structures.[5] Reflectivity changes in gas-exposed metal films have been reported with a modification

[a]Author to whom correspondence should be addressed; electronic mail: kkalli@cytanet.com.cy

 © 2002 American Institute of Physics

Downloaded 08 Dec 2007 to 194.42.23.6. Redistribution subject to AIP license or copyright; see http://jap.aip.org/jap/copyright.jsp

of the refractive index and, hence, the effective optical thickness of the film, through chemisorption and reaction.[6,7] Results have been obtained for the H–Pd system, where the formation of the PdH_x complex modifies the electron density of states in the near surface region of the metal.[8]

Metallic films may be classified as optically thick or thin. Optically thick refers to a thickness that exceeds the laser penetration depth at a given wavelength of light. Optically thin films represent the opposite condition. For optically thin films, one must account for the typically small penetration depth of the laser light in the metal film. For example, illumination of Pd at 633 nm gives a calculated penetration depth ($1/e$ value) of ~15 nm. Reflectivity measurements on films close to this thickness will be sensitive to effective thickness modifications as the phase shift of the light passing through the metal is affected, in addition to Fresnel reflection coefficient changes. For optically thick films, exposure to a reactive gas will modify surface properties with an accompanying change in the Fresnel coefficients, while changes in reflectivity arising from effective thickness modifications are considered very small.

Thin metal films have been studied to 6 nm, displaying a systematic deviation from bulk measurement. The electrical measurements reported by Frazier *et al.* became severely limited for film thicknesses below 25 nm as large cracks appeared.[4] Optical techniques are less sensitive to the island-like nature of the films, assuming the wavelength of light exceeds the mean island separation. On exposure to hydrogen, the islands can grow together forming larger structures, even growing in height by as much as ten times the original grain size, while significantly changing the surface coverage as the total volume of material is conserved. However, the change in coverage can still be very small compared with the wavelength of probing laser light, given the very small grain size. The probe beam will average over these regions on the order of the wavelength of light in all spatial directions.

We employ direct reflectivity measurements to study the interaction between Pd and hydrogen at room temperature. This approach offers a good signal-to-noise ratio, as the incident laser beam is completely amplitude modulated to allow for the generation of an electrical carrier signal, the amplitude of which is monitored using a lock-in amplifier, enhancing signal demodulation. This approach is entirely passive and nondestructive given the low optical power density of the probe beam. Note we do not have a surface specific technique, but rather a "bulk" measurement is made, as we obtain a measure of all the atoms within the sample. Hence, the results observed are those obtained as if the hydrogen atoms are uniformly distributed throughout the Pd layer. This does not pose a problem to our measurements as the hydrogen atoms rapidly diffuse into the metal with a diffusion time for an 8-nm film of ~1 μs, a value far shorter than the experimental time constants. The dominant rate-limiting step will be at the surface, as it is not atomically clean.

II. THIN FILM PREPARATION

The silicon wafers (p-type 5 ohms cm) were processed according to standard methods used to obtain gas sensitive catalytic metal–oxide–silicon devices.[9] The silicon dioxide wafers were oxidized in dry oxygen at 1100 °C to a thickness of 150 nm, the process was followed by a 15 min anneal in argon at the same temperature. The Pd films were deposited by thermal evaporation at a background pressure of about 10^{-7} Torr, for a deposition rate of 2–3 Å per second for all film thicknesses. The samples were kept at room temperature during the evaporation and no annealing of the film was performed before the measurements were made. The silicon nitride (Si_3N_4) films were grown to a thickness of 50 nm on a thermally grown oxide in dry oxygen, also of 50 nm thickness, by low pressure chemical vapor deposition.

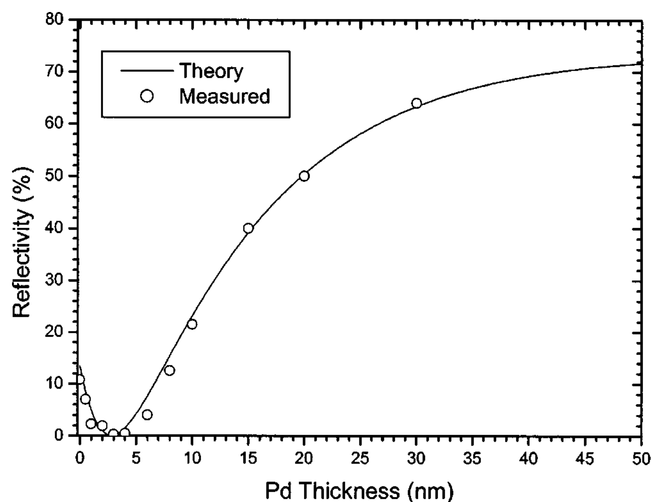

FIG. 1. Measured (open circles) and calculated (solid line) absolute reflectivity of the Pd/SiO_2/Si thin film structures as a function of the Pd-layer thickness. The bulk refractive index values of Pd have been used, taken from Ref. 12. Note the measurement error is contained within the data points.

III. EXPERIMENTAL RESULTS

The reflectivity of the as-deposited Pd films was measured in air. The films were stored at room temperature and pressure, but are stable under such conditions, as evidenced by AFM data. Furthermore, Pd is not easily oxidized; unless exposed to temperatures exceeding 80 °C. In Fig. 1, we observe the measured absolute reflectivity versus the thickness for Pd films deposited on SiO_2/Si. There is a decrease in reflectivity for films from 1 to 3 nm that reaches a minimum (almost zero %) close to 3 nm, after which the reflectivity increases reaching a plateau above 30 nm, at which point it is 64%, and approaching the bulk value for Pd metal (73%). Note that the solid line in Fig. 1 is the calculated reflectivity of the Pd/SiO_2/Si film, derived using the theory presented in Sec. IV. This data is characteristic of optically thin metal films prior to the chemisorption of a gas. The measurements are made on nonannealed samples, and the films have not reached their equilibrium morphology, therefore, the recorded reflectivity is characteristic of the as-deposited film. Moreover, this includes a substrate contribution, specifically the bare substrate (SiO_2/Si) has a reflectivity of 11%.

Changes in the reflectivity of the Pd films were monitored using a modulated laser beam reflected off the material surface. The samples were placed in a closed cell allowing

Downloaded 08 Dec 2007 to 194.42.23.6. Redistribution subject to AIP license or copyright; see http://jap.aip.org/jap/copyright.jsp

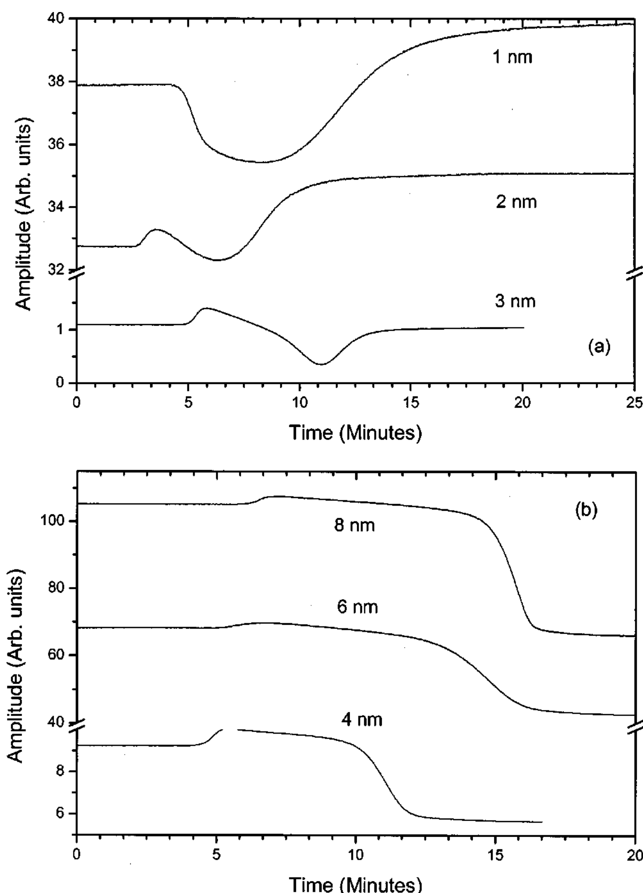

FIG. 2. The change in reflectivity for $Pd/SiO_2/Si$ thin films, varying in thickness from 1 to 8 nm, on first exposure to a concentration of 4% hydrogen gas in air. (a) The 1- and 2-nm samples undergo an inversion in the sample response, i.e., hydrogen/air exposure on further cycles leads to an increase/decrease in reflectivity. (b) The 4, 6, and 8-nm Pd films undergo a decrease/increase in reflectivity on further exposure to hydrogen air. The 3-nm sample eventually behaves in a similar manner to the thicker Pd films, once it has been stabilized after many hydrogen/air exposures.

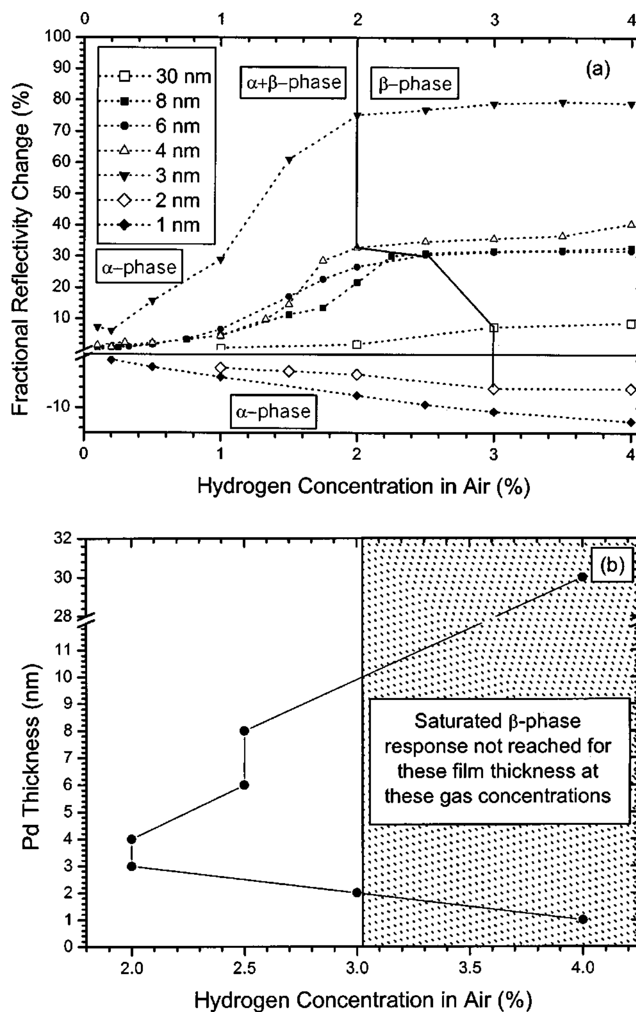

FIG. 3. (a) FCR of 1 to 30 nm $Pd/SiO_2/Si$ films, on exposure to hydrogen-in-air at 22 °C. For samples of thickness 3-nm and above, the hydrogen produces a decrease in reflectivity. 1- and 2-nm films produce an increase in reflectivity on exposure to hydrogen up to 4%. Fractional reflectivity change is defined as $(R_{\text{start}}-R_{\text{final}})/R_{\text{start}}$, hence, the FCR is negative for 1- and 2-nm samples. (b) The point at which the complete β-phase transition occurs has a complex dependence on Pd thickness.

for their response to various concentrations of hydrogen in balanced air to be measured. This method allows for basic studies of the interaction of the gases with the thin catalytic metal–insulator system. The system reached a saturated signal response before new gases or gas concentrations were introduced into the cell. Unless otherwise stated, the films were not annealed and measurements were made at 22 °C. Measurements are made at atmospheric pressures, therefore, the gas densities are high, $\sim 10^{19}$ molecules/m^3. For a sticking coefficient of one, the time for a complete adsorbate monolayer to cover the surface is $\sim 10^{-9}$ s. However, under standard temperature and pressure (STP) conditions the sticking coefficient in an inert atmosphere is reduced to 10^{-4} to 10^{-6}. In the presence of air, the surface is contaminated and hydrogen will coadsorb with other molecules increasing the reaction time by many orders of magnitude.

In Fig. 2, we present results for $Pd/SiO_2/Si$ samples, having nominal film thicknesses of 1, 2, 3, 4, 6, and 8 nm, on first and continued exposure to a 4% concentration of hydrogen gas in air. We note [Fig. 2(a)] that samples having a thickness less than 3 nm experience a reflectivity decrease that eventually recovers, reaching equilibrium at a signal level exceeding the original reflectivity. As a result, there is an "inversion" in the response of the film; i.e., exposure to subsequent hydrogen/air cycles produces a corresponding increase/decrease in reflectivity that is contrary to that recorded with thicker films. The 3-nm films lie at an intermediary position; a 27% fractional reflectivity increase is followed by a 75% reflectivity decrease, on initial hydrogen exposure. Under continued hydrogen exposure, the original reflectivity value is recovered and remains stable. Following many hydrogen/air cycles, the 3-nm film behaves in a similar manner to thicker films. For the same hydrogen exposure level, the 4, 6, and 8 nm films produce an increase in reflectivity that reach a maximum of 8.7%, 2.3%, and 2.3%, respectively, followed by a reflectivity decrease corresponding to a fractional reflectivity change of ~40%, 38%, and 37% [Fig. 2(b)]. The 4% hydrogen concentration coincides with a saturated response obtained from the thicker samples, for which the PdH_x complex lies in the β-phase.

In Fig. 3(a) we observe the fractional change in reflec-

Downloaded 08 Dec 2007 to 194.42.23.6. Redistribution subject to AIP license or copyright; see http://jap.aip.org/jap/copyright.jsp

tivity (FCR) as a function of hydrogen concentration for Pd/SiO_2/Si samples ranging from 1 to 30 nm thickness. All samples were first exposed to hydrogen concentrations of 4% in a balanced air mixture until a stable signal response was obtained. The hydrogen concentration level was systematically reduced to 0.2%. In between hydrogen exposures, the system was purged with a mixture of "synthetic air." This data has been classified in previous research into two groups, a flat response indicative of the β-phase, or a faster response associated with the α/β-mixed phase. There is also a distinct α-phase response, although it is not clear from this data, however, this is clarified in Sec. III A. At room temperature, the mixed phase compositions for α- and β-phases extend for a H/Pd ratio from 0.015 to 0.58.[1] The samples with a Pd thickness of 2 nm or greater display this characteristic behavior related to the two phases of the PdH_x complex. For hydrogen concentrations exceeding ~2% the slower response results from the slower compositional change of the β-phase PdH_x. Exposure to hydrogen concentrations below this level leads to a monotonic change in reflectivity that has a sharper response. It is interesting to note that the 1-nm sample does not undergo a mixed phase transition, responding linearly all the way to 4% hydrogen gas concentrations. This may be related to the very low coverage of the Pd film, for which there is not enough material present for the phase change to occur. This confirms the earlier findings of Kalli *et al.*[10]

The 0.58 H/Pd ratio constitutes the upper limit of the α/β-mixed phase composition at a temperature of 25 °C, as measured for Pd wires and powders.[1] From x-ray measurements, it has been determined that the upper limit of the α-phase composition, $\alpha_{\max}$, contributes to a lattice constant increase from 3.89 to 3.895 Å, i.e., an expansion of 0.13%. The β-phase concentration that co-exists with $\alpha_{\max}$, termed $\beta_{\min}$, results in a lattice constant of 4.025 Å.[1] Therefore, the lattice constant has increased by 3.5%; compared with pure Pd. Beyond the β-phase transition point, the contribution to the lattice constant increase is 0.37%, corresponding to 4.04 Å (up to a H/Pd ratio of 0.7). H/Pd=0.7 corresponds to the hydrogen content in equilibrium with a hydrogen pressure of one atmosphere (the maximum possible under STP conditions).[1] How we apply this knowledge to our samples requires care. It is not immediately obvious that the very thin Pd layers maintain the bulk (111) fcc structure and there may be deviations from bulk behavior, because of the small dimensions and also the influence of the supporting substrate, the latter issue is investigated in a later section. We note that the deposition process does not allow for a preferential crystalline axis of symmetry.

Figure 3(b) indicates that determining the point at which the complete β-phase transition occurs may not be a simple matter, with a complex dependence on Pd thickness indicated.[4,11] It appears to occur for a concentration of hydrogen gas from 2% to in excess of 4%, for the 3- to 30-nm thickness samples we examined. Furthermore, high hydrogen pressures are required to induce a β-phase transition for the 2-nm sample (3% hydrogen concentration), whereas the 1-nm sample does not reach the point of the β-phase transition.

The 3-nm film produces very large changes in the FCR, for all concentrations of hydrogen gas, because of the near zero absolute reflectivity at that Pd film thickness. Examples of the reflectivity response for 1- and 3-nm Pd/SiO_2/Si thin films are presented in Fig. 4. Note that the 1-nm sample undergoes a reflectivity increase during the hydrogen exposure and a decrease on the air cycling, the opposite is true for the 3-nm sample. The drift in the data results from morphological changes of the thin films when exposed to multiple hydrogen gas/air cycles. Figure 5 shows the actual reflectivity change with the square root of partial hydrogen gas pressure, complementing the data in Figs. 3 and 6.

Figure 6 shows the change in reflectivity versus the Pd-layer thickness on the SiO_2/Si substrate, for hydrogen concentrations up to 4%. As expected, thicker films produce a larger change in response (ΔR) to increasing hydrogen concentration levels, saturating beyond the 2% limit. It is important to note that the reflectivity change reaches a maximum level approaching the 30-nm thickness. This behavior is the result of two effects occurring with Pd samples of increasing thickness. The first corresponds to saturation in the absolute reflectivity values (Fig. 1), and the second has to do with the penetration depth of the Pd metal at the probing laser wavelength (which is estimated to be approximately the same, using the bulk refractive index values of Pd[12]). The change in

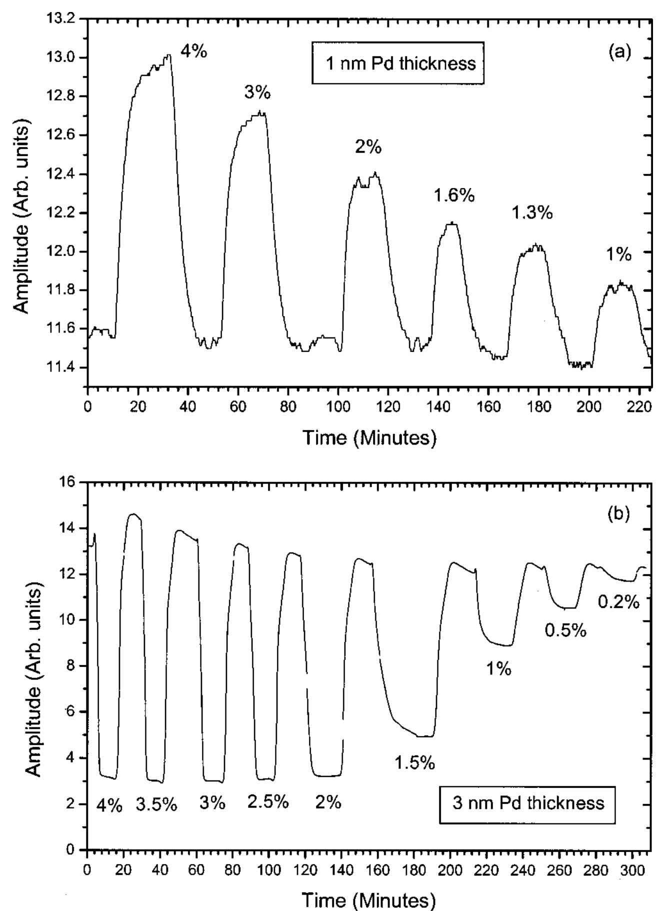

FIG. 4. Typical changes in reflectivity measured for (a) 1-nm and (b) 3-nm films. In (a) increases in reflectivity result from hydrogen exposure and decreases on purging with air, in (b) the opposite occurs. The hydrogen concentrations are marked.

Downloaded 08 Dec 2007 to 194.42.23.6. Redistribution subject to AIP license or copyright; see http://jap.aip.org/jap/copyright.jsp

reflectivity depends on the index of refraction change, which itself depends on the amount of hydrogen absorbed by the palladium. The observed signal however, depends on the amount of hydrogen seen by the probe beam. This in effect is the penetration volume of the laser beam in the Pd sample (assuming there is enough hydrogen to cover this volume). The maximum reflectivity change will occur at the maximum penetration volume. A comparison of 8-nm ($\Delta R/R = 33\%$) and 30-nm ($\Delta R/R = 8.6\%$) Pd films on SiO_2 (at 4% H_2 exposure) reveals a FCR ratio of 3.84. As the thickness of the samples is approaching the penetration depth of the laser, ΔR is approaching a common value for both samples, but displays a factor of 1.34 difference, as the 30-nm sample requires exposure to higher hydrogen concentrations for complete saturation. Therefore, the net difference (1.34×3.84) is equivalent to the ratio of the absolute reflectivity for 30- and 8-nm samples ($\sim 64/12.6 = 5.1$). This supports the reasoning that ΔR reaches a plateau as the Pd thickness increases beyond the penetration depth. The reflectivity measurements prove effective in studying effective thickness changes that affect the phase shift of the light passing through the metal. However, as the sample becomes thicker and a bulk material phase is entered, the reflectivity measurements are less adept at highlighting gas-induced changes, responding in main to changes in the Fresnel reflection coefficients.

We have highlighted the reflectivity change that occurs for thin Pd metal films on the SiO_2/Si support, when cycled in high gas concentrations. The data lies within a region in which α- and β-phases coexist. We need to determine the point at which the transition occurs between the three phases, namely α, mixed α/β, and β. We will now look, in detail, at what happens for the following two cases of gas cycling for an 8-nm sample. (i) The concentration of hydrogen gas in air is systematically lowered to 0.1%, i.e., an excursion into the β-phase has occurred and α_{max} has been exceeded, and (ii) the exposure is kept below the α-phase boundary and is systematically increased to α_{max} and beyond. We define parameters $\alpha_{concmin}$ and $\beta_{4\%}$ to represent stages in the α/β-phase corresponding to the minimum/maximum hydrogen concentration in air used, i.e., 0.1% and 4%, respectively.

A. Response of 8-nm Pd on SiO_2/Si: $\beta_{4\%}$ to α_{conmin}

The data in Fig. 7(a) details the behavior at low concentrations of hydrogen gas for an 8-nm Pd film. We note that below 1% hydrogen, Fig. 7(b), the response is very linear and shows that for the range covered, the sample demonstrates behavior according to Sievert's law which may be anticipated for this range of concentrations. There is no evidence of Langmurian behavior that has also been reported at low concentrations (to a 2000-ppm limit). This data strongly suggests that the sample lies in the α-phase only. The reflectivity change within the $\alpha + \beta$-mixed phase responds linearly to the introduction of hydrogen, whereas, Fig. 7(c) indicates that the data for concentrations exceeding α_{max}, i.e., purely in the β-phase, is tending to nonlinear behavior.

The response time required to reach equilibrium on hydrogen and air cycles is presented in Fig. 8, and is defined as that required to reach 10% and 90% of the maximum saturated value. On the air cycle, the response time decreases monotonically as the amount of hydrogen to be purged is reduced. On the hydrogen cycles, however, the data peaks for a concentration of ~1.8%, with a second peak at 0.64%. One would anticipate that under a concentration gradient, such as that existing between the hydrogen gas and Pd film, atoms diffuse from a high to a low concentration site obeying Fick's law. In this case, diffusion is driven by a chemical potential gradient that is a complex function of the concentration gradient, which itself depends on the properties of the Pd layer. Therefore, we tentatively hypothesize that the peaks in Fig. 8 mirror the points of maximum expansion of the crystal lattice in the α- and mixed-phase region, with the time taken for the system to reach equilibrium concomitantly increasing as the expansion of the lattice reaches a maximum. This is currently under further investigation.

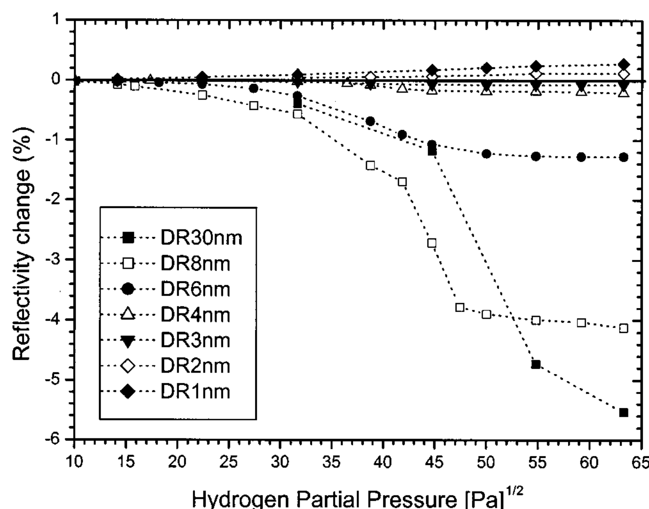

FIG. 5. The reflectivity change versus the square root of hydrogen partial pressure, showing that the β-phase transition occurs at 2% for 3- and 4-nm samples, and at 2.5% for 6- and 8-nm samples, and beyond 4% hydrogen concentration for the 30-nm sample.

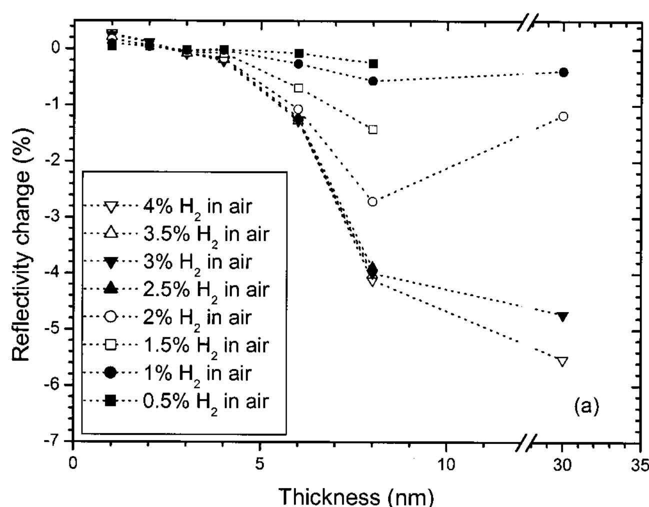

FIG. 6. Change in reflectivity of the Pd/SiO_2/Si films as a function of the Pd-layer thickness, for various concentrations of hydrogen gas in air at room temperature (22 °C). Films above 3-nm produce a negative change in reflectivity that saturates above 2% hydrogen.

Downloaded 08 Dec 2007 to 194.42.23.6. Redistribution subject to AIP license or copyright; see http://jap.aip.org/jap/copyright.jsp

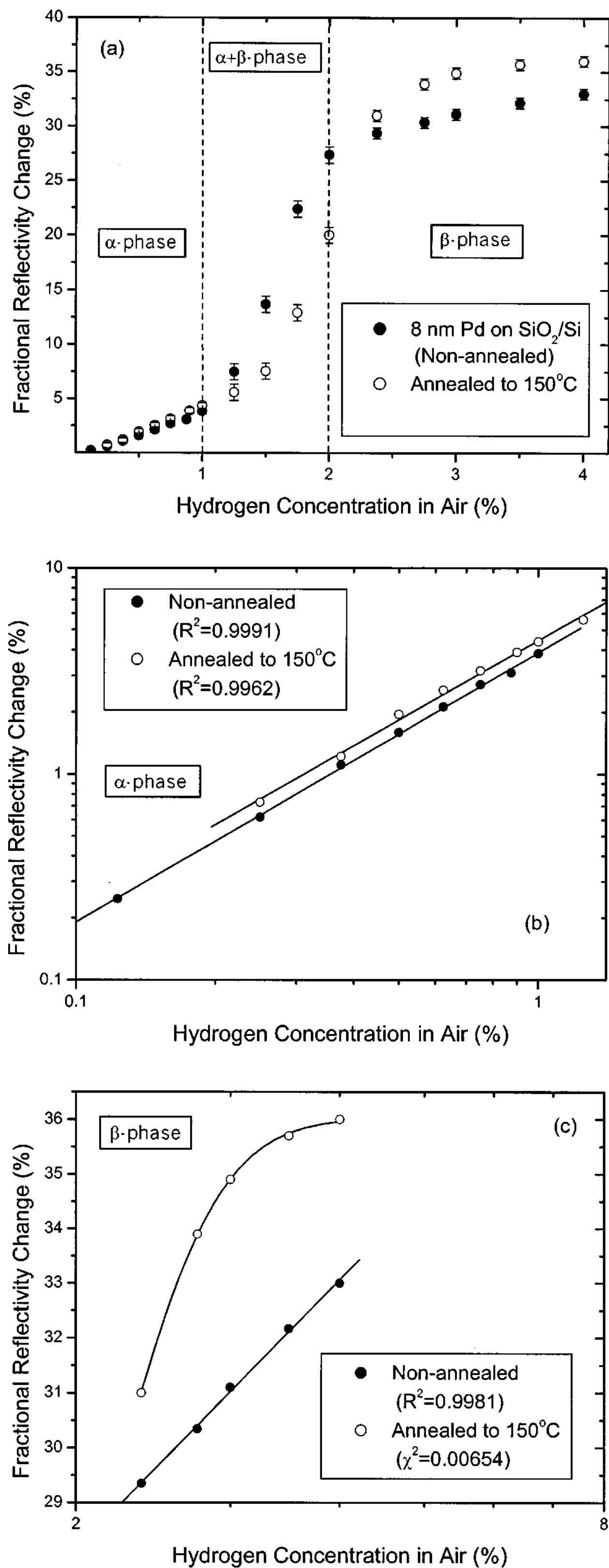

FIG. 7. Fractional change in reflectivity versus hydrogen concentration in air for nonannealed and pre-annealed 8-nm Pd samples, showing the different phase regions. (a) Complete range of data covering all phases. (b) α-phase shows good linearity and conformity to Sievert's law. (c) FCR within the β-phase showing a change in functional form of the pre-annealed Pd film characterized by a sigmoidal function. R^2 and χ^2 are correlation coefficients.

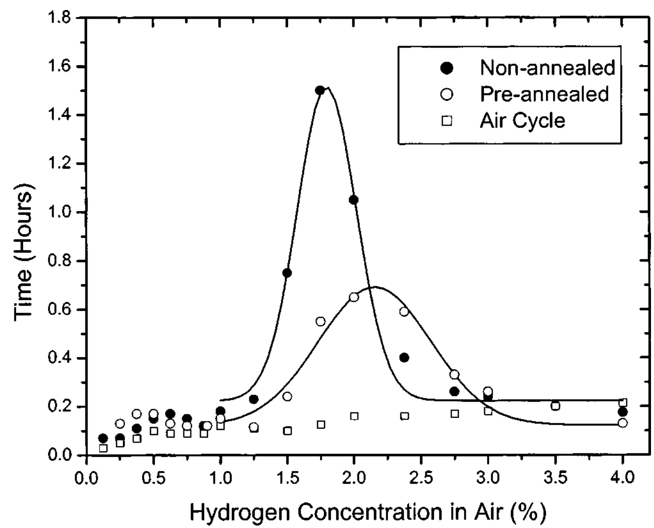

FIG. 8. Response time of non and pre-annealed 8-nm Pd on SiO_2/Si films as a function of hydrogen concentration in air. The response time for the nonannealed sample peaks at 1.8% hydrogen concentration, with a second peak at 0.64%. The pre-annealed sample peaks at 2.2% and 0.44%. The response time is reduced from 1.5 to 0.7 h for the pre-annealed film compared to the nonannealed film. (Gaussian fits are illustrative and limited between 1% and 4% hydrogen in air).

B. Response of 8-nm Pd on SiO_2/Si: $\alpha_{concmin}$ to $\beta_{4\%}$

8-nm Pd/SiO_2/Si films on first exposure to low concentrations of hydrogen gas in air have been studied to limit the primary response to the α-phase. In this case, we introduce hydrogen gas over extended periods of time (up to 100 h). We monitor the first- and fourth-order reflections from the sample, Fig. 9, therefore, we average over the hydrogen-induced morphological changes producing a more stable signal, while also being able to measure very small reflectivity changes. For the specific case of fourth-order reflections, the fractional reflectivity change is given by $\Delta R/R_4 = [1-(1-\Delta R/R_1)^4]$, where $\Delta R/R_1$ is the first-order fractional reflectivity change from the sample.

The first exposure of an 8-nm Pd/SiO_2/Si film to hydrogen concentrations well below the onset of the β-phase

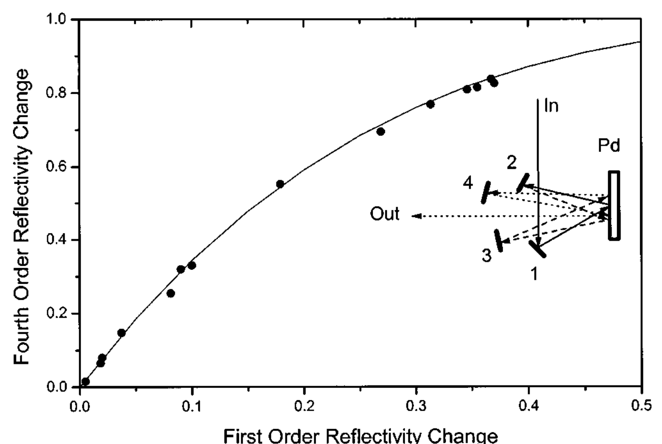

FIG. 9. The improvement in signal sensitivity obtained by measuring the fourth-order versus first-order fractional reflectivity change. The points correspond to actual data and the solid line is a plot of $\Delta R_4 = [1-(1-\Delta R_1)^4]$.

Downloaded 08 Dec 2007 to 194.42.23.6. Redistribution subject to AIP license or copyright; see http://jap.aip.org/jap/copyright.jsp

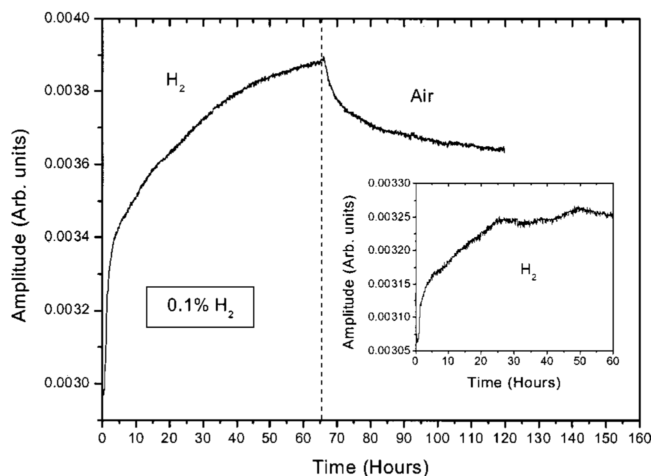

FIG. 10. Increase in signal for fourth- and first- (inset) order reflectivity for an 8-nm Pd film on SiO_2/Si, exposed to 0.1% hydrogen in air, showing that two rates of absorption are occurring.

(1000 ppm) leads to a rapid increase in reflectivity, Fig. 10. This increase does not saturate until exposure times exceeding 60 h, according to the first-order reflection (inset of Fig. 10). We observe a reflectivity increase of 31% for the fourth order (6.5%—first order), followed by a slow 8% recovery when the sample is re- exposed to balanced air. If the equilibrium rates for absorption and desorption are the same, one would anticipate that after a 60 h exposure to air, the sample would reach equilibrium with a reflectivity maintained at the level measured prior to hydrogen exposure.

Clearly, this is not the case here and indicates that the hydrogen gas remains bound to the Pd lattice. One possible reason for this is because oxygen at the surface prevents the hydrogen from escaping through the formation of hydroxyl groups. However, we believe that this binding of hydrogen is not permanent in the α-phase, as the reflectivity does eventually reach its original value, for example, exposure to 1% hydrogen (at the apparent limit of the α-phase) resulted in a reflectivity recovery after two days in air at room temperature.

Anecdotal evidence for the observed changes in reflectivity is given in Fig. 11. An initial reflectivity increase is always observed, and reaches a maximum value, after which a reflectivity decrease is recorded on continued hydrogen exposure. The decrease occurs rapidly once exposure levels exceed 0.2% hydrogen. For example, Fig. 11(a) indicates the response of a fresh sample exposed to 0.3% hydrogen in air, and shows that an increase in peak fourth- (first-) order reflectivity of 32% (7.5%) after 13 h that is followed by a very slow decrease over several days. Figures 11(b) and 11(c) show representative data for exposure to hydrogen concentrations of 0.75% to 2%, (measurements were made from 0.1% to 4% hydrogen), a fresh 8-nm sample was used for each hydrogen concentration. For hydrogen concentrations up to 1%, the reflectivity increase is followed by a slow decrease on continued exposure that reaches saturation well short of the start value. Exposure levels of 2% hydrogen are required to produce the decrease in reflectivity (30% first order) on a par with that observed in Fig. 2. Moreover, once

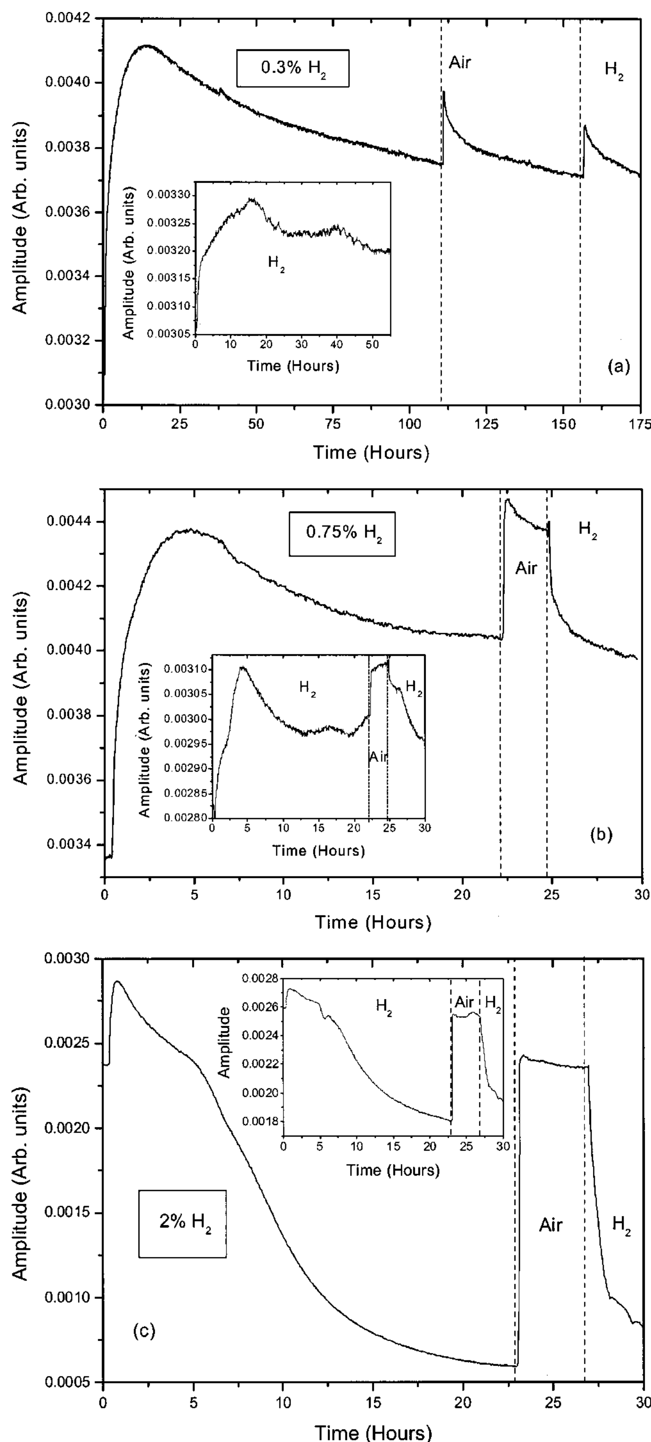

FIG. 11. Reflectivity as a function of time for 8-nm Pd/SiO_2/Si films exposed to various concentrations of hydrogen in air and air under STP conditions. (a) 0.3% hydrogen in air, (b) 0.75% hydrogen in air, (c) 2% hydrogen in air.

a steady-state signal has been reached on the hydrogen cycle, purging with air initially produces a sharp *increase* in reflectivity, after which the signal approaches the steady-state response, this is clear in Fig. 11(a). For higher hydrogen concentrations, the sample was not allowed to reach the equilibrium level and hydrogen was reintroduced into the system, resulting in behavior mirroring that observed on the air cycle for Fig. 11(a), with the decrease in reflectivity tak-

Downloaded 08 Dec 2007 to 194.42.23.6. Redistribution subject to AIP license or copyright; see http://jap.aip.org/jap/copyright.jsp

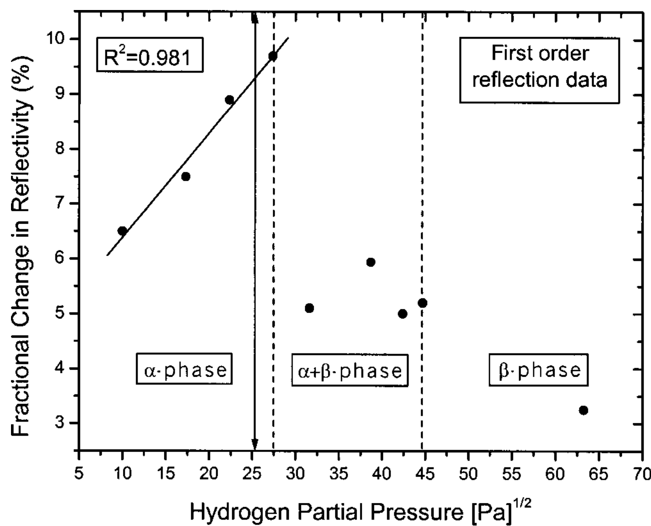

FIG. 12. Measured FCR versus the square root of hydrogen partial pressure in air (0.1%–4%). The solid line is a least square fit to the data for hydrogen partial pressures less than 0.75%; this corresponds to a range over which the α-phase hydride is dominant and the formation of the β-phase hydride is prohibited. The arrow indicates where the peak in response time in the α-phase lies, from Fig. 8.

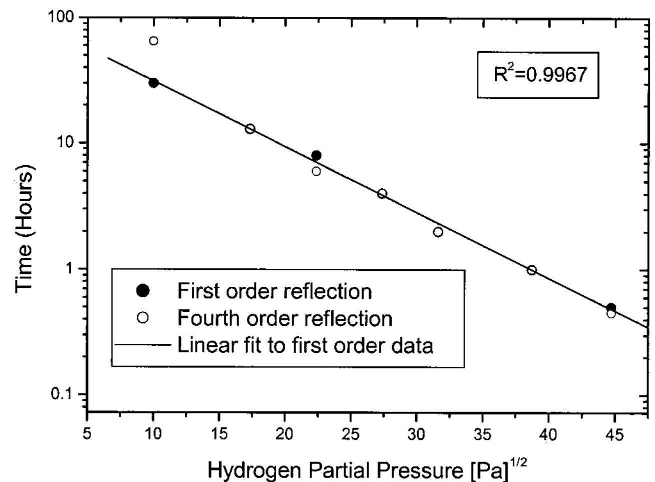

FIG. 13. Time required for the 8-nm $Pd/SiO_2/Si$ samples to reach their maximum reflectivity on first exposure to varying concentrations of hydrogen gas in air, at room temperature (0.1% to 2%). The solid line is a least squares fit to the data recovered from the first-order reflection and indicates that for both first- and fourth-order reflection data the hydrogen partial pressures are proportional to the logarithm of time.

ing a similar time. However, for concentrations of 0.75% and above, the decrease in reflectivity on the hydrogen cycle is notably accelerated. This data should be compared with that of when the $Pd/Si/SiO_2$ samples were first exposed to hydrogen levels at 4% (β-phase), for which hydrogen and air cycles decreased and increased the FCR, respectively.

To discover more about the nature of the initial increase in reflectivity, we examined its dependence on the partial pressure of hydrogen gas, as shown in Fig. 12. The graph displays good linearity for hydrogen concentrations less than 0.75%, for which the FCR gives a measure of the amount of hydrogen absorbed into the Pd film and indicates that Sievert's law is holding. Increasing the hydrogen concentration above 0.75% leads to a reduction in the fractional increase in reflectivity, which tends to a value of ~3%, where it remains constant. This departure from linearity indicates the onset of a mixed α- and β-phase region at room temperature. However, note that this does not quite coincide with the data recovered once $\beta_{4\%}$ has been exceeded, where an indication of a mixed-phase response is given only once a 1% hydrogen concentration is surpassed. The difference between the two points of transition may relate to the relaxation of built-in strain within the metal film during deposition that is relaxed on gas cycling only at high concentrations. For the case of first exposure to hydrogen gas levels within the α-phase, the lattice has not reached its maximum expansion level. Furthermore, we have evidence that hydrogen remains within the Pd lattice once $\beta_{4\%}$ has been reached, therefore, it appears that there are two routes to equilibrium which depend on the initial hydrogen exposure level. It should also be noted that the hydrogen concentration at the transition point of the α-phase in Fig. 12 is close to the peak in the response time of Fig. 8 that lies within the α-phase region, and is marked by an arrow in Fig. 12.

In Fig. 13, we observe the time to reach the initial maximum reflectivity values on first exposure to hydrogen in air. There is no sign of complex behavior and the hydrogen partial pressure is proportional to time according to

$$\log(t) = Kp(H_2)^{1/2}. \quad (1)$$

C. Discussion

Our data need careful interpretation, as it could be perceived that the samples always displaying a reflectivity decrease following the excursion into the β-phase are permanently transformed into a β-phase composition. We believe that the hydrogen is irreversibly absorbed into the film at room temperature if the concentration exceeds the β-phase boundary. We have noted that the FCR, following gas cycling above $\beta_{4\%}$ levels, falls by a few percent over several days in air (for the 8-nm film, this drop is ~7%), and the original value is not recovered, at least at room temperature. We have also noted that moderate heating of the sample (temperature excursions of 30 °C) results in temperature-induced reflectivity changes that return to the modified reflectivity level. When the film is subsequently exposed to 1% hydrogen, the reflectivity level drops in keeping with much of the data once $\beta_{4\%}$ has been exceeded. However, annealing in air at 160 °C for 1 h induces an increase in reflectivity returning to the original room temperature value prior to hydrogen exposure. Re-exposing this annealed film to 1% hydrogen induces an *increase* in reflectivity, similar to the data in Fig. 11. However, the FCR is far smaller at 1.2% and the response time is significantly faster at 7 min. Regardless, the film behaves in a manner broadly similar to a virgin film. The smaller changes in FCR on both hydrogen and air cycles can be explained by strain release and the rearrangement of dislocation networks, induced by the high temperature excursion. This implies that once $\beta_{4\%}$ is exceeded at room temperature, hydrogen remains bound to the metal film for long periods of time, certainly over a period of a few weeks, whereas the stability to moderate heating indicates that this

Downloaded 08 Dec 2007 to 194.42.23.6. Redistribution subject to AIP license or copyright; see http://jap.aip.org/jap/copyright.jsp

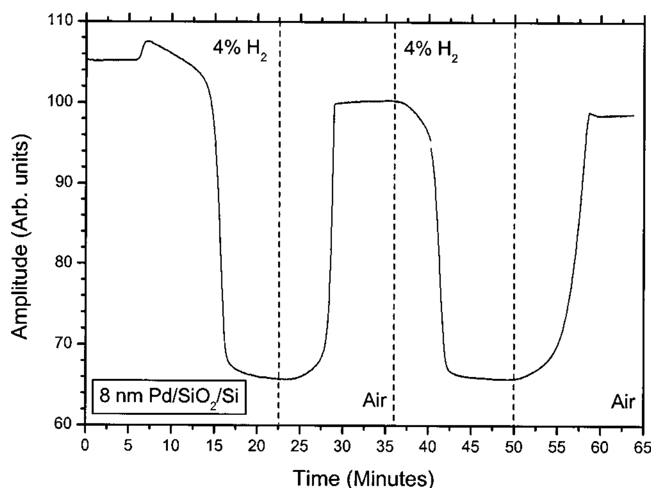

FIG. 14. Typical reflectivity changes demonstrated by an 8-nm Pd on SiO_2/Si on hydrogen cycling.

stability may hold for several months. This phenomenon may be evidence of hysteresis in the response of the very thin films; this is under further investigation. Furthermore, this may explain the following observations that are always recorded for the behavior of the thicker Pd films on SiO_2/Si regarding the first exposure to hydrogen gas, Fig. 14.

Observation (1): On first hydrogen exposure, the reflectivity initially increases, and if α_{max} is exceeded, decreases until a saturated signal level is reached that is not consistent with hydrogen desorption alone.

Explanation (1): Increases and decreases in reflectivity on the first hydrogen exposure are linked to the phase state of the Pd metal, associated with the α- and β-phases, respectively. If $\beta_{4\%}$ is reached, the sample is converted into a β-phase structure that remains stable at room temperature.

Observation (2): On continued cycling, the increase in reflectivity observed on the first hydrogen cycle fades to zero.

Explanation (2): A complete transition to the β-phase occurs as $\beta_{4\%}$ is reached and α_{max} is exceeded, minimizing any contributions from the α-phase.

Observation (3): There is a gradual decrease in overall reflectivity that stabilizes after several hydrogen/air cycles.

Explanation (3): The Pd lattice retains a small proportion of the absorbed hydrogen, maintaining a stable β-phase structure at room temperature. Heating the sample to high temperatures can remove the trapped hydrogen atoms.

D. Pre-annealing at 150 °C

When the Pd is annealed (150 °C for 1 h) *prior* to hydrogen exposure, we note that exposure to 1% hydrogen in air produces an increase in reflectivity of ~1.5% and a rapid response time of 2 min, in contrast to nonannealed films. There are strong similarities between this data and that recovered when the thin film was heated to remove hydrogen. Following a system purge with air, exposure to 4% hydrogen produces a decrease in reflectivity; of near identical magnitude to before (34%), but without any initial increase in reflectivity that we have associated with the α-phase and the response time is fast at ~6 min. Regardless, these observations suggest that the role of lattice disorder, or defect distribution, may be more important to the initial α-phase response than to the β-phase. To obtain a qualitative and semiquantitative measure of this effect, we repeated our previous gas cycling studies on the pre-annealed film, cycling from 4% to 0.1% hydrogen. Figure 7(a) compares the data between non- and pre-annealed samples, clearly showing a difference in behavior. The pre-annealed sample shows an extended α-phase transition at close to 1.4% hydrogen, although the gradient in this phase region remains unchanged, Fig. 7(b). The most distinctive behavior results in the β-phase region, where there is a definite change in functional form for the Pd response. In the pre- annealed case, the data are best fit by a sigmoidal function, Fig. 7(c) inset, for a range of hydrogen concentration, from 2.25% to 4%, where the sample is well into the β-phase. Indeed, a good sigmoidal fit is obtained for data between 1% and 4% hydrogen, inclusive. Fitting over the same range for the nonannealed sample produced a poor fit. The response time is presented in Fig. 8. The comparison between non and pre-annealed films indicates an improved response time on the annealed sample, reduced from 1.5 to 0.7 h, and a shift in the peak response time to ~2.2% and 0.44%. This shift mirrors the increase in the transition point to the β-phase, Fig. 7(a). This is in keeping with our earlier hypothesis, of coincidence with points of maximum expansion of the crystal lattice.

IV. REFLECTIVITY CHANGES ON HYDROGEN EXPOSURE

Two effects occur when Pd films, greater than 2-nm thickness, are exposed to hydrogen; an initial reflectivity increase associated with hydrogen charging of the material in the α-phase, and a subsequent reflectivity increase or decrease on further exposure to high concentrations of hydrogen. We now show that the reflectivity increase or decrease is associated with a composite nature of the thin-film devices; a change related to the modification of the reflection amplitude at the various gas–metal, metal–insulator interfaces, and the phase shift of the light as it passes through the metal film. The adsorbed and absorbed hydrogen may affect the phase shift by either modifying the thickness of the film, the refractive index, or a combination of both effects.

In order to explain the observed reflectivity changes, in particular, the reflectivity inversion effect, we consider a simple one-dimensional model that describes the Pd/SiO_2/Si thin-film structure, as presented in Fig. 15. We use a classical model that ignores surface scattering and roughness effects; AFM data indicates that for the Pd/SiO_2/Si films, this is an acceptable assumption as the roughness is on a spatial scale far smaller than the wavelength of light. The reflection amplitude for the thin-film structure is described by[13]

$$r=\frac{r_1+r_2e^{-i\varphi_1}+r_3e^{-i(\varphi_1+\varphi_2)}+r_1r_2r_3e^{-i\varphi_2}}{1+r_1r_2e^{-i\varphi_1}+r_1r_3e^{-i(\varphi_1+\varphi_2)}+r_2r_3e^{-i\varphi_2}}, \quad (2)$$

where r_i is the reflection amplitude for the corresponding interface, according to Fig. 15, and ϕ_i is the phase shift of

Downloaded 08 Dec 2007 to 194.42.23.6. Redistribution subject to AIP license or copyright; see http://jap.aip.org/jap/copyright.jsp

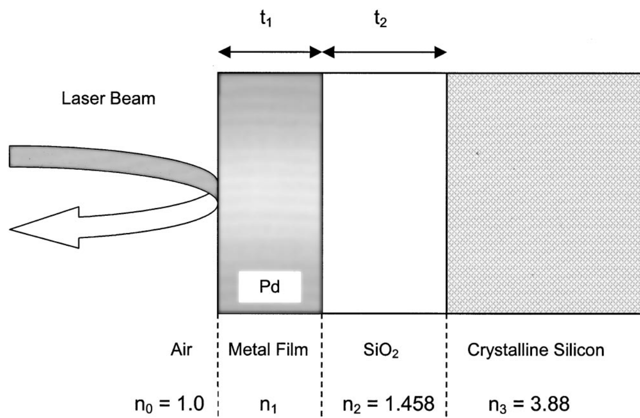

FIG. 15. Schematic diagram showing the thin film configuration used to model the reflectivity change of the Pd/SiO_2/Si structure. The refractive indices n_i refer to the gas, Pd metal, SiO_2, and silicon, for $i=0-3$, respectively. The thicknesses are t_1 for the Pd film, and t_2 for the SiO_2 layer.

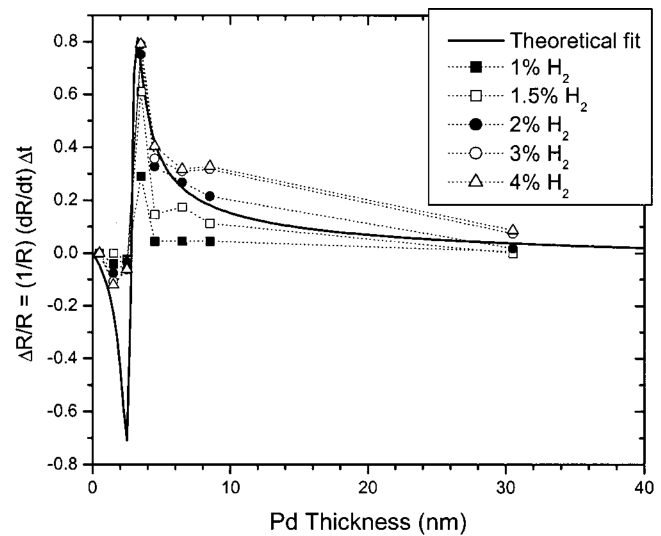

FIG. 16. Comparison of the measured FCR ($\Delta R/R$) for the various film thicknesses of Pd on SiO_2/Si, for different hydrogen gas concentrations, with $(1/R)(dR/dt)\Delta t$ derived from the theoretical curve of Fig. 1. The variable Δt is adjusted to optimize the fit (in this case to 2% hydrogen) and is set as a percentage change of the original film thickness.

the light as it passes through the metal and insulator layers. The Fresnel reflection amplitudes are given by

$$r_1=(n_0-n_1)/(n_0+n_1),$$
$$r_2=(n_1-n_2)/(n_1+n_2), \tag{3}$$
$$r_3=(n_2-n_3)/(n_2+n_3)$$

and the phase shift in regions 1 and 2 are

$$\varphi_1=4\pi n_1 t_1/\lambda \quad \text{and} \quad \varphi_2=4\pi n_2 t_2/\lambda, \tag{4}$$

where λ is the wavelength of light, n_i and t_i the appropriate refractive index (where necessary complex), and thickness of the film, respectively, and the index $i=0$, 1, 2, 3 refers to air, Pd metal, SiO_2, and crystalline silicon, respectively. The accumulated phase shift through the metal film is more accurately written as

$$\varphi=\frac{4\pi}{\lambda}\int_0^t n_1(x)dx. \tag{5}$$

Within the limits of this model, the Pd layer is modified through changes in the Fresnel reflection amplitudes and the phase of the light through the metal film. In order to justify the use of Eqs. (2)–(4), we assume that the entire reflectivity change is associated with a change in the phase shift alone, as the perturbation of reflection amplitude and the phase shift through the metal are mutually dependent. Furthermore, the phase shift that results from variations in n_1 throughout the metal film is indistinguishable from a constant n_1 and a change in film thickness Δt (an *effective* thickness change that is required to produce the observed reflectivity). We do not have a surface- or indeed subsurface-specific technique, therefore, this lack of measurement sensitivity to the exact location and nature of the changes in electronic structure can be expressed as an equivalent change in the Pd metal film thickness. The change in phase shift can be written as

$$\Delta\varphi=\frac{4\pi}{\lambda}\int_t^{t+\Delta t} n_1(x)dx=\frac{4\pi}{\lambda}n_1\Delta t. \tag{6}$$

Taking the derivative of the absolute reflectivity with respect to thickness, $(1/R)(dR/dt)$, as a function of film thickness, one can relate the FCR caused by the change in $\Delta\phi$ to the change in thickness. This can be expressed as

$$\Delta R/R=(1/R)(dR/dt)\Delta t. \tag{7}$$

In this way, the measured FCR is proportional to the change in reflectivity with respect to thickness, with the constant of proportionality being the effective change in Pd thickness.

One may question the validity of this approach as it has been reported that for the H–Pd system, there is a change in the carrier concentration at the SiO_2/Si interface and this may impact the measurements for the thinnest Pd films. Simulating the changes at this interface indicate no noticeable changes in the functional form of the fitting curve, with a small change in the theoretical effective thickness of the sample. Indeed, in Fig. 16, we observe that the model predicts the increase in the reflectivity for the thin samples, as witnessed by the negative FCR for the 1- and 2-nm samples for all hydrogen concentrations.

We take $(1/R)(dR/dt)$ solely from the data in Fig. 1. Figure 16 gives a typical example of the measured FCR, that is $\Delta R/R$, and the corresponding $(1/R)(dR/dt)\Delta t$, which is taken from the theoretical fit of Fig. 1. The value of Δt is set as a percentage change in the *effective* thickness of the Pd film, incorporating both refractive index and thickness changes. Therefore, if we adjust Δt to equate both sides of Eq. (7) as a function of the hydrogen concentration, for the different thicknesses of Pd, we arrive at Fig. 17. Note that the data points for the thick samples, 3-nm and more were used to optimize the fit. The data in Fig. 17 can be taken as purely illustrative and show a trend for the film thicknesses that undergo a β-phase transition. The fit is optimized for the samples exceeding 3-nm and therefore the β-phase transition point is biased. Nevertheless, the reflectivity changes can indeed be described by the *effective* thickness change (including refractive index contributions) that affects the phase of

Downloaded 08 Dec 2007 to 194.42.23.6. Redistribution subject to AIP license or copyright; see http://jap.aip.org/jap/copyright.jsp

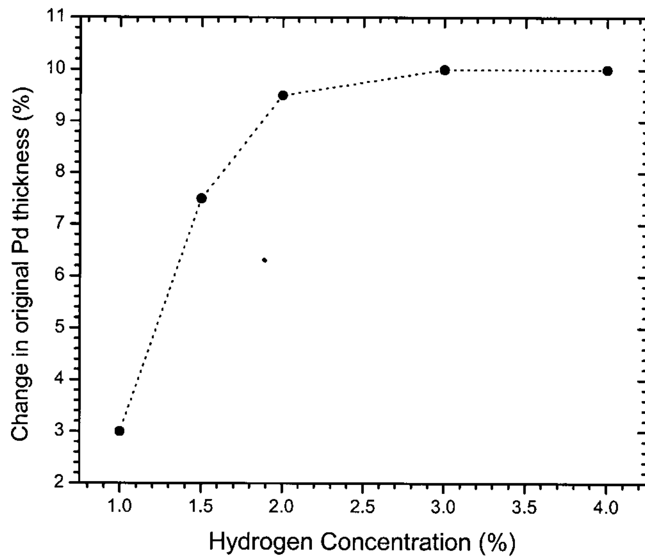

FIG. 17. Percentage change in thickness for the $Pd/SiO_2/Si$ samples exposed from 1% to 4% hydrogen gas in air. Δt is the fitting parameter used to equate both sides of Eq. (7). The data are indicative of the trend in response as the samples undergo the β-phase transition and is intended purely for illustrative purposes. The FCR can be described by an effective thickness change of the Pd layer that also incorporates refractive index contributions, without recourse to changing the Fresnel reflection coefficients.

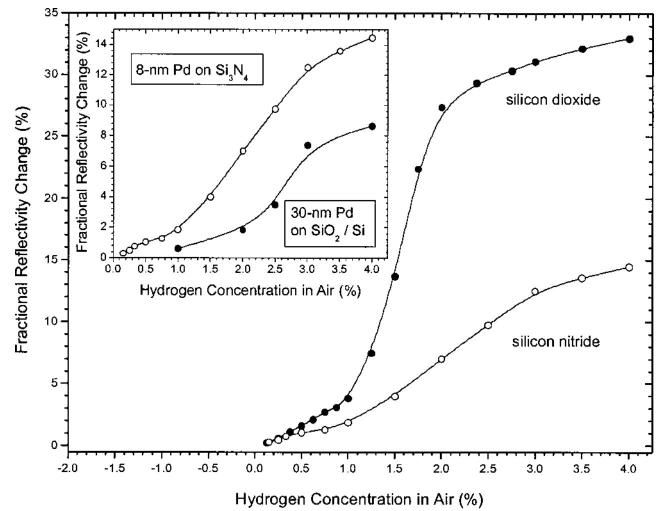

FIG. 18. Fractional reflectivity changes for different concentrations of hydrogen for 8-nm Pd thin films on the different substrates. The curve in the upper left-hand side corner compares the behavior of the 8-nm Pd film on Si_3N_4 with the 30-nm Pd film on SiO_2/Si and indicates that neither film has undergone a β-phase transition at the given levels of hydrogen exposure. We surmise that the Pd on Si_3N_4 has undergone morphological changes that have increased the effective thickness of the sample.

the light passing through the film, without recourse to modifying the Fresnel reflection coefficients. The thickness change resulting from the modifications to the lattice constant corresponds to ~3% when the Pd has been exposed to high hydrogen concentrations.[1] Figure 17 indicates that the effective thickness change is nearer 10%, therefore the refractive index contribution to the FCR on hydrogen exposure accounts for approximately three times the contribution associated with any thickness change alone.

V. ATOMIC FORCE MICROSCOPY

Figure 18 shows the reflectivity change with hydrogen concentration for the two substrates. The silicon dioxide sample has the largest FCR (33%), whereas the silicon nitride sample has not been completely transformed into the β-phase (15% FCR). Based on our earlier findings, the transition point to the β-phase is dependent upon the Pd thickness, and the data suggest that the sample has increased in thickness. Comparison with the 30-nm sample indicates that the thickness of the silicon nitride sample has increased to a similar level, Fig. 18 inset. However, the total amount of Pd is conserved and therefore the data can result if there is a redistribution of metal, on a length scale between clusters that is less than the wavelength of the probing laser beam. AFM images of 8-nm $Pd/SiO_2/Si$ show small structural features with a height of <1 nm, after 4% hydrogen gas cycling. Prior to cycling and on the bare silicon dioxide substrate, the AFM image is essentially featureless.

Images from 8-nm Pd samples on silicon nitride show pronounced structural changes following hydrogen exposure. Unexposed films, with relatively small (<5 nm) structural features [Fig. 19(a)], are transformed to structures with diameters of ~100 nm and height ranging between 80–100 nm, Fig. 19(b). These images were collected several weeks after hydrogen exposure, and given the stability of the sample in the β-phase, the morphological changes are considered semipermanent. The large nanometer structures have on average a thickness that exceeds the penetration depth of

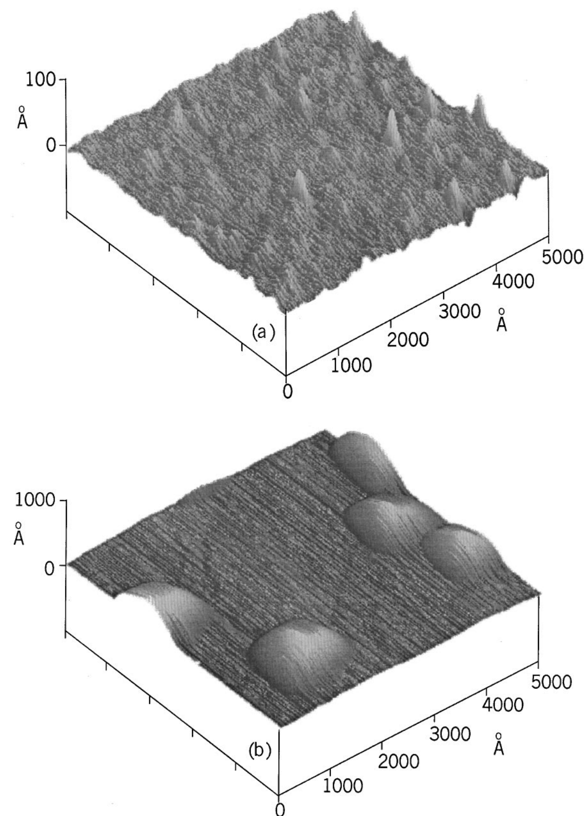

FIG. 19. AFM pictures of the 8-nm Pd film evaporated on silicon nitride: (a) before and (b) after hydrogen exposure at 4%.

Downloaded 08 Dec 2007 to 194.42.23.6. Redistribution subject to AIP license or copyright; see http://jap.aip.org/jap/copyright.jsp

the probing beam. This suggests that only a small fraction of the hydrogen absorbed by the Pd nanostructures is detectable. This agrees with the reduced FCR for this substrate in comparison with the silicon dioxide and the shift in the point of transition to the β-phase that more closely resembles the 30-nm sample.

VI. DISCUSSION

The interaction of hydrogen and Pd at room temperature in air proceeds through large compositional changes of the PdH_x complex, with small variations in the gas phase concentration of hydrogen producing large changes in reflectivity. For high hydrogen concentrations, the chemisorption of gases on the surface occurs rapidly and results in a reflectivity change that alters the refractive index (and hence, optical thickness) of the film and the Fresnel reflection coefficients, the former being the dominant contributor. This results from having a laser penetration depth that is of the same order as the metal thickness.

A potentially intractable problem is determining the nature of the Pd structure, because the samples are very thin, and may therefore deviate from bulk (111) fcc Pd, and because of the role of the rather distinct substrate types. The deposition process does not allow for a preferential crystalline axis of symmetry. There is reasonable evidence that for Pd exceeding one monolayer, corresponding to $\sim$0.22 nm, the structure becomes characteristic of bulk (111) fcc Pd. Indeed, Strongin *et al.*[14] have shown that for Pd layers of 1.3–1.4 monolayers (0.3 nm), the structural change to fcc (111) is complete; rapid hydrogen uptake is particularly associated with the (111) fcc Pd structure. We have also evidenced that consistent uptake of hydrogen by $Pd/Si/SiO_2$ films only occurs when the Pd layer exceeds 0.5 nm. A 0.1 nm sample was highly inactive and this can reasonably be explained by the inability to form the fcc (111) structure.[10] This is important and suggests that hydrogen uptake by Pd is not an atomic property, but has a strong dependence on the structure of the Pd layer, that may itself be biased by the substrate–metal interaction. That hydrogen uptake is greater for dense Pd layers points to a critical role on the local electronic structure. This can be inferred from the AFM data, where the Pd distribution on the SiO_2/Si is denser than that for Si_3N_4, the latter of which form clustered Pd peaks with mean separations far greater than the Pd mean free electron path. The direct reflectivity data mirrors this finding, and the $Pd/SiO_2/Si$ film proves far more useful in eliciting a reflectivity change on hydrogen exposure. Particularly interesting results are derived from the Pd deposited on the silicon nitride films. The FCR data implies a large increase in the Pd film thickness, as indicated by the shift to greater hydrogen concentrations for the β-phase transition point and the reduced FCR magnitude; this is confirmed by AFM measurements where changes to surface energy effects result in the creation of nanostructures. While the α- and β-phases are solid solutions of hydrogen in the Pd interstitial sites, the formation of long range ordered structures is known to occur at high concentrations and low temperatures. These structures are formed on subsets of interstitial sites and are consistent with nearest neighbor repulsive interactions. In our case, the Pd deposition occurs at room temperature on as-deposited films that have not reached their equilibrium morphology. Gas cycling changes the morphology, with the Pd withdrawing from the silicon surface as the surface energy of the system changes. It has been documented that Pd films display poor adhesion to SiO_2 and Si_3N_4 substrates, with delamination and blistering occurring. The AFM data suggests that there is a redistribution of Pd into clusters, and that the role of blistering is not predominant.

There is a limit to the amount of hydrogen that the α-phase can store, and this is apparent when samples are first exposed to high hydrogen concentrations that lie in the β-phase. An initial increase in reflectivity peaks and then falls to a level that can not be explained by desorption alone. Associating the reflectivity increases with the α-phase follows from the Pd film exposure to low levels of hydrogen, from which a Sievert's law relation is derived. This is evidence for solution of hydrogen in Pd in an atomic form.

The response time of Pd films in the β-phase differs markedly from samples of the same thickness in the α-phase. The former is characterized by a profile that peaks at a point coincident with the β-phase transition, the latter by a logarithmic dependence of time with the square root of hydrogen partial pressure. Annealing experiments reveal differences between non and pre-annealed Pd samples, indicating departures for the α- and β-transitions points and the functional form in the β-phase. This may be expected as hydrogen interacts with solutes and lattice defects, both of which act as traps or low energy sites. The presence of unsaturated traps decreases the effective diffusivity of hydrogen, as is the case for low hydrogen concentrations. However, under high hydrogen concentrations, the defect or solute traps are saturated and the diffusivity is not greatly affected by their presence. When the Pd is heated to high temperatures, the traps are removed affecting the response of the Pd film. To conclude, laser reflectivity measurements have proven useful in eliciting information regarding the fundamental properties of thin Pd films.

[1] F. A. Lewis, *The Palladium/Hydrogen System* (Academic, London, 1967), and references therein.
[2] Y. Fukai, *The Metal-Hydrogen System*, Springer Series in Material Science Vol. 21 (Springer-Verlag, Berlin, 1993).
[3] J. F. Lynch and T. B. Flanagan, J. Phys. Chem. **77**, 2628 (1973).
[4] G. A. Frazier and R. Glosser, J. Less-Common Met. **74**, 89 (1980).
[5] R. Jansson, H. Arwin, M. Armgarth, and I. Lundström, Appl. Surf. Sci. **37**, 44 (1989).
[6] M. A. Butler and A. J. Ricco, Appl. Phys. Lett. **53**, 1471 (1988).
[7] M. A. Butler and A. J. Ricco, Sens. Actuators **19**, 249 (1989).
[8] M. A. Butler, J. Electrochem. Soc. **138**, L46 (1991).
[9] A. Spetz, U. Helmersson, F. Enquist, M. Armgarth, and I. Lundström, Thin Solid Films **177**, 77 (1989).
[10] K. Kalli, A. Othonos, C. Christofides, A. Spetz, and I. Lundström, Rev. Sci. Instrum. **69**, 3331 (1998).
[11] M. W. Lee and R. Glosser, J. Appl. Phys. **57**, 5236 (1985).
[12] P. B. Johnson and R. W. Christy, Phys. Rev. B **9**, 5056 (1974).
[13] H. Anders, *Thin Films in Optics* (Focal, New York, 1967).
[14] M. Strongin, M. El-Batanouny, and M. A. Pick, Phys. Rev. B **22**, 3126 (1980).

Downloaded 08 Dec 2007 to 194.42.23.6. Redistribution subject to AIP license or copyright; see http://jap.aip.org/jap/copyright.jsp